Plastic changes in amygdala subregions by voluntary running contribute to exercise-induced hypoalgesia in neuropathic pain model mice

Katsuya Kami[1,2] [iD], Fumihiro Tajima[2] and Emiko Senba[2,3]

Abstract

Physical exercise has been established as a low-cost, safe, and effective way to manage chronic pain, but exact mechanisms underlying such exercise-induced hypoalgesia (EIH) are not fully understood. Since a growing body of evidence implicated the amygdala (Amyg) as a critical node in emotional affective aspects of chronic pain, we hypothesized that the Amyg may play important roles to produce EIH effects. Here, using partial sciatic nerve ligation (PSL) model mice, we investigated the effects of voluntary running (VR) on the basal amygdala (BA) and the central nuclei of amygdala (CeA). The present study indicated that VR significantly improved heat hyperalgesia which was exacerbated in PSL-Sedentary mice, and that a significant positive correlation was detected between total running distances after PSL-surgery and thermal withdrawal latency. The number of activated glutamate (Glu) neurons in the medal BA (medBA) was significantly increased in PSL-Runner mice, while those were increased in the lateral BA in sedentary mice. Furthermore, in all subdivisions of the CeA, the number of activated gamma-aminobutyric acid (GABA) neurons was dramatically increased in PSL-Sedentary mice, but these numbers were significantly decreased in PSL-Runner mice. In addition, a tracer experiment demonstrated a marked increase in activated Glu neurons in the medBA projecting into the nucleus accumbens lateral shell in runner mice. Thus, our results suggest that VR may not only produce suppression of the negative emotion such as fear and anxiety closely related with pain chronification, but also promote pleasant emotion and hypoalgesia. Therefore, we conclude that EIH effects may be produced, at least in part, via such plastic changes in the Amyg.

Introduction

Increase in physical activity levels can inhibit the onset of life-style related diseases, such as metabolic syndrome, cardiovascular disease, diabetes, cancer and psychiatric disorders including depression and anxiety. In addition to these positive effects of physical activity, many clinical and animal studies over past 30 years verified effectiveness of physical activity as a non-pharmacological intervention to improve pain, and it has been well known that voluntary running (VR) or treadmill running in neuropathic pain (NPP) and inflammatory pain (IFP) model animals significantly improves pain-related behaviors such as mechanical allodynia and heat hyperalgesia (exercise-induced hypoalgesia: EIH).[1–3] As potential

mechanisms of EIH effects, previous studies suggest impacts of multiple events, including marked alterations in cytokines, neurotrophins, neurotransmitters, and

[1]Department of Rehabilitation, Wakayama Faculty of Health Care Sciences, Takarazuka University of Medical and Health Care, Wakayama, Japan
[2]Department of Rehabilitation Medicine, Wakayama Medical University, Wakayama, Japan
[3]Department of Physical Therapy, Osaka Yukioka College of Health Science, Ibaraki, Japan

Corresponding Author:
Katsuya Kami, Department of Rehabilitation, Wakayama Faculty of Health Care Sciences, Takarazuka University of Medical and Health Care, 2252 Nakanoshima, Wakayama City, Wakayama 640-8392, Japan.
Email: k-kami@tumh.ac.jp

endogenous opioids in injured peripheral nerves, dorsal root ganglia, spinal dorsal horns and the brainstem following physical exercise.[3]

On the other hand, recent neuroimaging analysis in chronic pain patients demonstrated that dysfunction of the mesocortico–limbic system including the ventral tegmental area (VTA), amygdala (Amyg), hippocampus (Hipp), nucleus accumbens (NAc) and medial prefrontal cortex (mPFC) plays critical roles in the development and maintenance of chronic pain, which provided an important clue to elucidating novel mechanisms underlying EIH effects. Our recent study demonstrated that VR produces EIH effects and reverses the marked reduction in activated lateral VTA (lVTA)-DA neurons induced by NPP. The proportions of activated laterodorsal tegmental nucleus (LDT)-cholinergic and lateral hypothalamus-orexin neurons were significantly enhanced by VR.[4] These results suggested that EIH effects may be produced, at least in part, by activation of the mesolimbic reward system.

The amygdala is a limbic brain region that plays a key role in emotional processing, neuropsychiatric disorders, and the emotional-affective dimension of pain. The amygdala is also a node constituting the mesocortico-limbic system, and is comprised of different nuclei, namely, the basolateral nuclei of amygdala (BLA), central nuclei of amygdala (CeA) and the intercalated cells (ITC) located between them. Animal studies reported that neuronal excitability is enhanced in the CeA in acute arthritis and neuropathic pain, and in the BLA in an acute arthritis pain model.[5] The CeA is further divided into three subdivision, the capsular division of CeA (CeC), lateral division of CeA (CeL) and medial division of CeA (CeM). The BLA is a complex consisting of the lateral amygdala (LA) and the basal amygdala (BA), which is further divided into the lateral BA and medial BA. The amygdala receives cortical (mPFC, ACC, IC) and thalamic inputs that provide polymodal sensory information to the BLA.[6] Nociceptive information from the peripheral tissues projects into the parabranchial nucleus (PBN) via the spinal dorsal horn, and then PBN neurons directly input into the CeC.[7] Beyeler et al.[8] indicated that BLA neurons projecting to the NAc (BLA-NAc) respond to a reward-predictive cue, whereas BLA neurons projecting to the CeM (BAL-CeM) are excited by an aversive stimulation including pain. They also reported that the BLA-CeM and BLA-NAc projectors are densest in the latBA and medBA, respectively.[9] By using optogenetic techniques, Cai et al.[10] indicated that activation of PBN-CeA circuit is sufficient to cause behavior of negative emotion, such as anxiety, depression and aversion, while activation of the BLA-CeA pathway reduces anxiety and depression, and induces behavior of reward.

Since a growing body of evidences implicated the amygdala as a critical node in emotional affective aspects of pain, we hypothesized that constituent elements of the amygdala, the CeA and BLA may play important roles to produce EIH effects in a different way each other. In this study, we investigated the effects of VR on glutamate (Glu) neurons in the BA and gamma-aminobutyric acid (GABA) neurons in the CeA in neuropathic pain model mice. In addition, we also investigated whether the BA neurons projecting to the NAc lateral shell are activated by physical exercise. The present study provided evidences that both extinction of negative emotions and promotion of pleasant emotion which induced by plastic changes in amygdala altered by VR may be critical events to produce EIH effects.

Materials and methods

Preparation of NPP model mice

Adult C57BL/6J mice were used in this study. Neuropathic pain (NPP) model mice were prepared by partial sciatic nerve ligation (PSL).[11] Under deep anesthesia, approximately one-third to one-half of the sciatic nerve at the right mid-thigh level was tightly ligated with 8-0 silk sutures. Sham operations were performed using the same procedures described above excluding PSL. All experiments in this study were approved by the Animal Care Committee of Wakayama Medical University (Ref. No. 910). All experiments conformed to the National Institutes of Health Guide for the Care and Use of Laboratory Animals (NIH Publication No. 99-158, revised 2002).

Experimental groups and the VR protocol

Mice were divided into six groups: 1) Naive-Sedentary mice (n = 6), 2) Naive-Runner mice (n = 6∼8), 3) Sham-Sedentary mice (n = 6), 4) Sham-Runner mice (n = 6∼8), 5) PSL-Sedentary mice (n = 6∼10) and 6) PSL-Runner mice (n = 6∼10). All Runner and Sedentary mice were placed in individual cages equipped with a running wheel or locked running wheel under a 12/12-hour light-dark cycle, and Naive-, Sham- and PSL-Runner mice were allowed to run freely on the running wheel. Since running exercise in the early stage after nerve injury is an important requirement to induce significant EIH effects, mice were returned to the cage equipped with a running wheel so that they can voluntarily run immediately after PSL-surgery. The VR protocol is shown in Figure 1(b). All mice, except for Naive mice, performed VR for 2 weeks prior to the sham operation or PSL. PSL and Sham mice were returned to individual cages immediately after surgery, and running
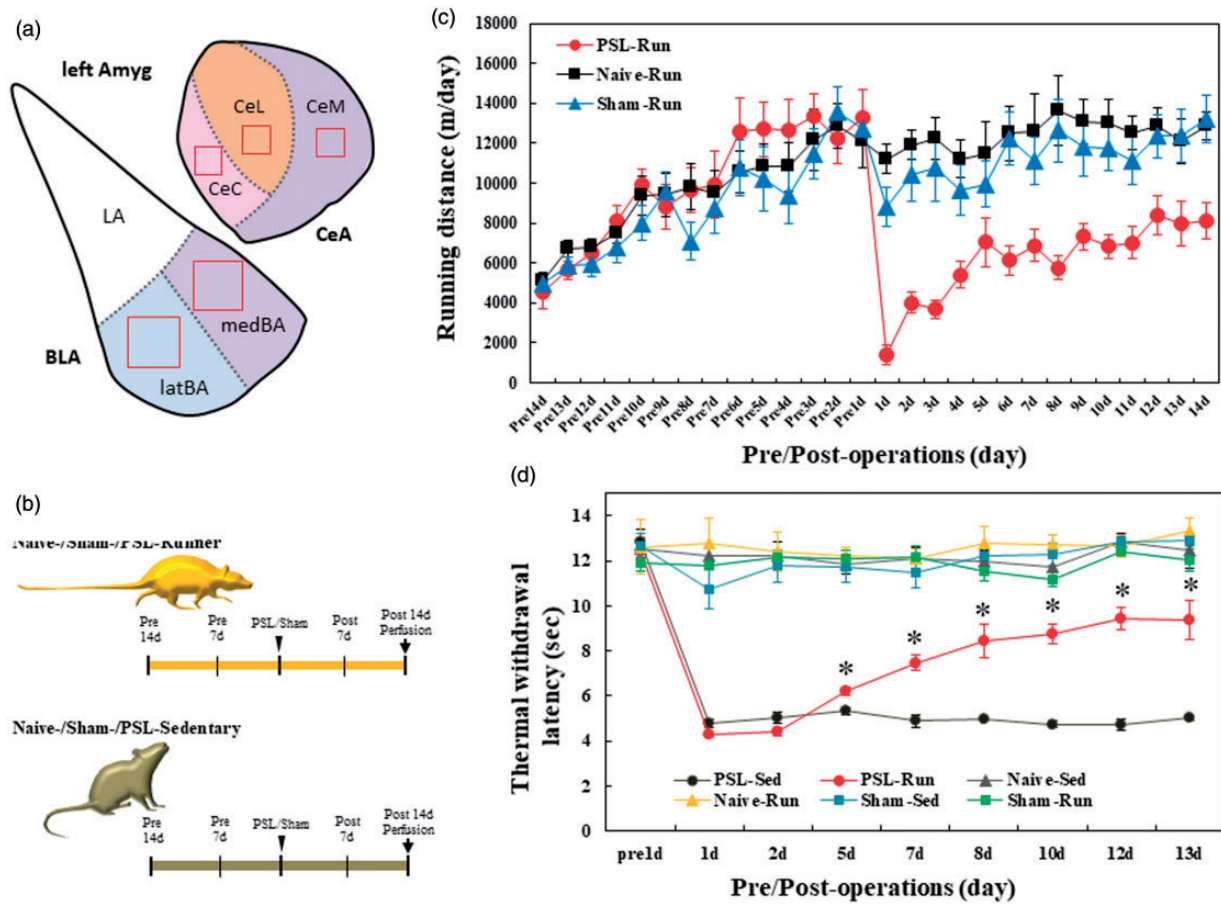
Figure 1. Schematic drawing of the amygdala, and changes in running distances and pain behavior during the experimental period. (a) Schematic drawing of the amygdala. The amygdala is a complex consisting of the basolateral nuclei of amygdala (BLA), central nuclei of amygdala (CeA) and the intercalated cells (ITC). The CeA is further divided into three subdivisions, the capsular division of CeA (CeC), lateral division of CeA (CeL) and medial division of CeA (CeM). The BLA consists of the lateral amygdala (LA) and the basal amygdala (BA), and the latter is further divided into the lateral BA and medial BA. The red squares indicate areas in which immunoreactive neurons were counted. (b) Protocol of VR. Naive-Runner, Sham-Runner and PSL-Runner mice were placed in individual cages equipped with a low-profile wireless mouse running wheel, being allowed to run freely on it. Sedentary mice were reared in cages with a locked running wheel. (c) Changes in running distances of three groups of Runner mice (n = 6). (d) Plantar tests were performed for all experimental groups. Thermal withdrawal latencies were significantly higher in PSL-Runner mice than those in PSL-Sedentary mice (*p < 0.01, n = 6).

distances were measured during the 14-day period before and after the surgery. The rotations ran on the running wheel/hour were monitored using a magnetic reed switch attached to a computerized exercise-monitoring system (SOF-860 wheel manager software, MED Associates, Inc.), and daily running distances (m/day) and diurnal variation in running distance (m/hour) were calculated using the number of rotations on the running wheel.

Evaluation of pain behavior

In order to abolish diurnal variation in pain behaviors, plantar tests were performed at 8:00 a.m. Prior to plantar test, mice were placed in an acrylic glass enclosure with a wire mesh bottom ($8.3 \times 8.3 \times 8.0$ cm) and

allowed to acclimate for 30 min. Heat hyperalgesia was evaluated by the plantar test, which measures withdrawal latency (sec) to a radiant thermal stimulus delivered from beneath the glass floor to the plantar surface of the hindpaw (Plantar Test, Model7371, Ugo Basile, Comerio, Italy). The heat stimulus by the projector lamp bulb was focused on the plantar surface of the ipsilateral hindpaw, and the minimum time (sec) needed to evoke quick withdrawal of the paw by heat stimulation was taken as the withdrawal latency.[12] The plantar test was performed three times for each mouse, and mean values were considered as the withdrawal latency. In all behavioral evaluations, the investigator was blinded to the experimental groups in order to avoid any bias.

Immunofluorescence analysis

The primary antibodies were as follows: FosB (mouse monoclonal antibody, dilution 1:2000, Abcam, ab11959), glutamic acid decarboxylase 67 (GAD67) (goat polyclonal antibody, dilution 1:1000, Abcam, ab80589), Calcitonin Gene Related Peptide (CGRP) (rabbit polyclonal antibody, dilution 1:500, Sigma, PC205L) and EAAC1 (rabbit polyclonal antibody dilution 1:1000, Sigma).

Mice were perfused transcardially with 4% paraformaldehyde in 0.1 M phosphate-buffered saline (PBS), and the brain was post-fixed. After cryoprotection, the brain was frozen using dry ice-cooled hexane. Serial 25-μm thick brain sections including the BA (Bregma -2.18 mm~-1.46 mm) or CeA (Bregma -1.46 mm$\sim$ -0.94 mm) in the coronal plane were mounted serially on slides. After blocking for non-specific staining, sections for dual immunofluorescence staining were incubated simultaneously with two kinds of primary antibodies diluted in 0.1 M PBS containing 5% normal donkey serum and 0.3% Triton X-100 at 4°C for 48 hours. Then, sections were incubated with the secondary antibodies diluted in 0.1 M PBS containing 5% normal donkey serum and 0.1% Triton X-100 during overnight at 4°C. The secondary antibody used for the detection of GAD67 immunoreactivity was Alexa Fluor 594- or 405-labeled donkey anti-goat (1:500, Abcam, ab150136 or ab175665). The secondary antibody used for the detection of FosB immunoreactivity was Alexa Fluor 488-labeled donkey anti-mouse IgG (1:500, Abcam, ab150109). The secondary antibodies used for the detection of CGRP and EAAC1 immunoreactivities were Alexa Fluor 405- or 488-labeled donkey anti-rabbit IgG, respectively (1:500, Abcam, ab175648 or ab150061). Sections were washed in 0.1 M PBS and mounted in Vectashield mounting medium with DAPI (H-1200, Vector Labs., Burlingame, CA). Fluorescence signals were detected using a confocal microscope (LSM700, Carl Zeiss, Oberkochen, Germany) equipped with an argon-helium laser. Negative control sections, which were processed without primary antibodies, had no significant positive immunoreactivity.

Quantitative analysis of immunopositive neurons

Immunofluorescence images of the BA on the ipsilateral and contralateral sides were acquired at a magnification of 10 x. A square of 200 μm × 200 μm in size, as shown in Figure 1(a) for the medBA and latBA, was placed on the microscope images using LSM Image Browser 4.2 (Carl Zeiss, Germany), and the number of immunopositive cells within the square was counted. On the other hand, immunofluorescence images of the CeA on the ipsilateral and contralateral sides were acquired at a magnification of 20×. A square of 100 μm × 100 μm in size, as shown in Figure 1(a) for the CeA subdivisions, was placed on the microscope images using LSM Image Browser 4.2 (Carl Zeiss, Germany), and the number of immunopositive cells within was counted. The mean value of three randomly selected sections from six sections per brain was regarded as the value of immunopositive neurons per mouse. In order to avoid any bias in the results of the quantitative analysis, investigators were blinded to all experimental groups throughout quantitative analyses.

Injection of retrograde tracer into the NAc lateral shell, immunofluorescence staining and quantitative analysis

Mice performed VR for 2 weeks prior to injection of the retrograde tracer, and were then placed in a stereotaxic apparatus. Unilateral injection of Retrobeads Red (RBR) (50 nl, Lumafluor Inc., Naples, FL) was performed by inserting a microsyringe into the left side of the NAc lateral shell (Bregma: anteroposterior,1.0 mm; mediolateral, 1.5 mm; and dorsoventral, -5.0 mm). RBR-injected mice were returned to their individual cages, and the running distance was recorded for 2 weeks before and after injection. The brains of RBR-injected Runner mice were processed in the same manner as described for the Immunofluorescence analysis. To evaluate RBR-injection sites, 35-μm thick brain sections including the NAc lateral shell were mounted serially, and after briefly rinsing with PBS, slides were mounted in Vectashield mounting medium with DAPI.

The same immunostaining procedure for the FosB immunostaining in the BA was adapted for RBR-injected brain sections. Immunofluorescence images of the BA on the administrated sides of the RBR were acquired at a magnification of 10 x. A square of 200 μm × 200 μm in size, as shown in Figure 1(a) for the medBA or latBA, was placed on the microscope images using LSM Image Browser 4.2 (Carl Zeiss, Germany), and the number of RBR-positive cells and the number of dual positive cells for the RBR signals and FosB immunoreactivity within the square was counted. The total number of cells in three randomly selected sections from six sections per RBR-injected Runner mouse was regarded as the value of immunopositive cells. In order to avoid any bias in the results of the quantitative analysis, investigators were blinded to all experimental groups throughout quantitative analyses.

Statistical analysis

Quantitative data are presented as the mean ± standard error of the mean (SEM). A repeated measures ANOVA

followed by Bonferroni's post hoc test was used to compare withdrawal latency among the experimental groups. Multiple comparisons of the number of immunopositive cells among experimental groups were performed using a one-way ANOVA followed by Bonferroni's post hoc test. Comparison of the number of RBR positive cells between the medBA and latBA was performed using a student's t-test. Differences were considered to be significant at $p < 0.05$.

Results

Changes in running distances and pain behaviors

The manner of exercise by experimental animals is classified into forced exercise, such as treadmill running and swimming, and VR such as free running on a running wheel. Especially, there are many studies that indicated the improvement of emotion with VR in pain research using experimental animals. It is indicated that VR in inflammatory pain model mice improves perception, emotion and cognition deteriorated with chronic pain.[13] VR increases dopamine levels in the mPFC, and enhances the performances of cognitional task that is regulated in the mPFC.[14] In addition, Picher et al. reported that both inflammatory pain and stresses in animal model were attenuated by VR.[15] VR also improves symptoms of chronic stress such as depression and anxiety-like behaviors.[14–20] In addition, since VR can produce positive emotion via activation of the brain reward system, the results mentioned above indicate that VR can activate vigorously mesocortico-limbic system including brain reward system. Therefore, in the present study, VR, but not forced exercise, was loaded on mice to elucidate relationship between Amyg and EIH effects.

Figure 1(c) shows changes in running distances per day by Naive, Sham, and PSL-Runner mice. The mean running distance in the three groups was approximately 5000 m/day on day 1 after the start of the experiment (Pre14 d), and running distances markedly increased by day 14 (Pre1 d) (Naive-runner: 12127.85 ± 1363.17 m/day; Sham-Runner: 12720.22 ± 718.9 m/day; PSL-Runner: 13277.62 ± 1408.69 m/day). The running distance by Sham-Runner mice decreased to 8808.72 ± 961.77 m/day on day 1 post-surgery (1 d), but returned to nearly pre-surgery levels by day 6 post-surgery (12234.27 ± 1336.97 m/day: 96.2%). On the other hand, the running distance by PSL-Runner mice markedly decreased on day 1 post-surgery (1385.39 ± 488.23 m/day: 10.4%). However, these values gradually increased thereafter. The running distance by PSL-Runner mice recovered to approximately 61% (8093.41 ± 913.68 m/day) of the pre-surgery level by day 14

post-surgery (14 d). These changes were consistent with our previous results.[4]

We performed plantar tests to evaluate the effects of VR on heat hyperalgesia (Figure 1(d)). No marked differences were noted in the pre-operative data of withdrawal latencies among mice assigned to the six experimental groups. Furthermore, Runner mice in the Naive and Sham groups exhibited no significant alterations in withdrawal latencies throughout the experimental period, indicating that VR had no effects on sensory sensitivity in mice without PSL. PSL-Sedentary mice had markedly shorter withdrawal latency (4.78 ± 0.195 sec) at 1 days after PSL than at pre-surgery (withdrawal latency: 12.8 ± 0.558 sec), and these decreased latencies were maintained throughout the experimental period. Withdrawal latencies were significantly longer on day 5 in PSL-Runner mice (6.21 ± 0.169 sec, $p < 0.01$) than in PSL-Sedentary mice (5 days $= 5.32 \pm 0.158$ sec). Furthermore, significant increases in withdrawal latencies were observed until day 13 after PSL in PSL-Runner mice (11.37 ± 0.759 sec, $p < 0.01$) compared with those in PSL-Sedentary mice (5.0 ± 0.09 sec). Taken together with our previous findings,[4] the present results confirmed that the pain behaviors in NPP model mice were significantly improved by the VR protocol employed in the present study.

We next examined the relationships between the threshold of final pain on behavioral tests (13 d) and total running distances during the 13-day period after PSL in PSL-Runner mice. We found a significant positive correlation between total running distance and withdrawal latency (Figure 2(a); $R = 0.805$, $n = 10$, $p < 0.01$). These results also confirmed our previous findings.[4] Interestingly, however, when we examined the relationships between the threshold of final pain on behavioral tests (13 d) and total running distances during the experimental period in PSL-Runner mice, no significant correlation was verified (Figure 2(b); $R = 0.323$, $n = 10$), meaning that the levels of physical activity after nerve injury are closely involved in an extent of NPP.

PSL- and VR-induced changes in the latBA- and medBA-Glu neurons

Neuronal type constituting the BA is largely Glu neurons (~80%), and exist also slightly GABA neurons (~20%).[21,22] When dual immunostaining used EAAC1 (a marker for Glu neurons) and GAD67 (a marker for GABA neurons) performed, we found neuronal type accordance with previous observations (Figure 3(A)). In addition, immunoreactivity of FosB was used as a marker of activated neurons because FosB protein gradually accumulates in response to chronic stimuli, including wheel running, and persists for long periods of time because of its high stability.[23] The BA, which is
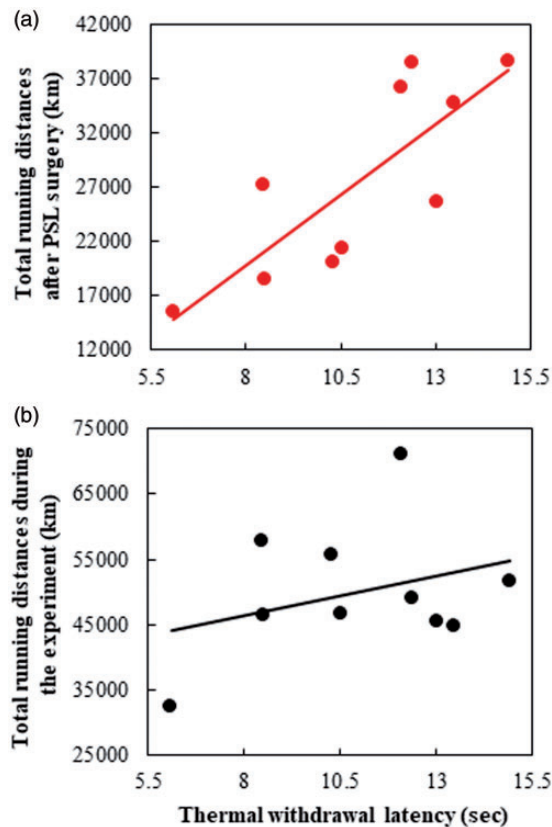
Figure 2. Relationship between thermal withdrawal latency and total running distances in PSL-Runner mice. (a) A significant positive correlation was observed between total running distances after PSL-surgery and the thermal withdrawal latency in PSL-Runner mice ($R = 0.805$, $n = 10$, $p < 0.01$). (b) No significant correlation was detected between the thermal withdrawal latency and total running distances during the experimental period in PSL-Runner mice ($R = 0.323$, $n = 10$, N.S.).

composed of anatomically and functionally heterogeneous Glu neuron subpopulations with different axonal projections, is divided into two parts: the latBA and medBA. A previous study suggested that the latBA neurons projecting to the CeA may be the primary subpopulation of Glu neurons that are preferentially activated by aversive stimuli, including chronic pain, whereas the medBA neurons projecting to the NAc lateral shell may primarily signal reward and salience.[9] To elucidate a difference in activation of Glu neurons in both latBA and medBA, we immunostained the brain sections containing the BA with FosB and GAD67 antibodies, and thereby FosB$^+$ neurons without the immunoreactivities for GAD67 were considered as the Glu neurons.

Typical immunostained images of activated BA neurons in PSL-Sedentary and PSL-Runner mice were showed in Figure 3(B), and the numbers of activated Glu neurons in the latBA and the medBA on the

ipsilateral and contralateral sides were compared among each group (Figure 3(C)). The area of the BA in which the quantitative analysis was made, was indicated in Figure 1(a). In agreement with the images of photomicrographs, the numbers of activated Glu neurons (GAD67$^-$ FosB$^+$) in the Sham- and PSL-Sedentary mice were significantly higher in the latBA compared with those in the medBA ($p < 0.01$). In contrast, the numbers of activated Glu neurons in the Naive-, Sham- and PSL-Runner mice were significantly higher in the medBA compared with those in the latBA ($p < 0.01$). There were no significant differences between the ipsilateral and contralateral sides in all groups.

When the relationship between the total running distance during the 14-day period after surgery in PSL-Runner mice and the number of activated Glu neurons (sum of both the ipsilateral and contralateral sides) in PSL-Runner mice was examined, a significant positive correlation was noted (Figure 3(D), $R = 0.813$, $n = 6$, $p < 0.05$).

PSL- and VR-induced changes in the CeA-GABA neurons

The CeA contains largely GABA neurons,[24–26] and further is divided into three subdivisions, the CeL, CeM and CeC. The CeC, especially is strongly immunostained with CGRP antibody, because the CGRP-containing neurons in the PBN directly project into the CeC.[27] Therefore, we identified the CeC as both CGRP and GAD67-immunopositive regions, and the CeM and CeL were identified in accordance with The Mice Brain Atlas.[28] The squares put on the CeM, CeL and CeC in Figure 1(a) indicate the area in which the quantitative analysis was made.

Using dual immunostaining with GAD67 and FosB antibodies, we found significantly many GAD67$^+$ neurons with FosB$^+$ immunoreactive nuclei on both the ipsilateral and contralateral sides of the CeM, CeL and CeC in PSL-Sedentary mice (Figure 4(a)) compared with those of PSL-Runner mice (Figure 4(b)). When the number of activated GABA (GAD67$^+$ FosB$^+$) neurons on the ipsilateral and contralateral sides in the CeC (Figure 4(c)), CeM (Figure 4(d)) and CeL (Figure 4(e)) were compared, consistent with the immunostaining images, the numbers were significantly higher in PSL-Sedentary mice than those in all other groups ($p < 0.01$). No significant differences between the ipsilateral and contralateral sides were observed in all groups.

When the relationship between the thermal withdrawal latency and the number of activated GABA neurons (sum of both the ipsilateral and contralateral sides) in PSL-Runner mice was examined, we found significant negative correlations in the CeC (Figure 4(f), $R = 0.848$, $n = 6$, $p < 0.05$), the CeM (Figure 4(g),
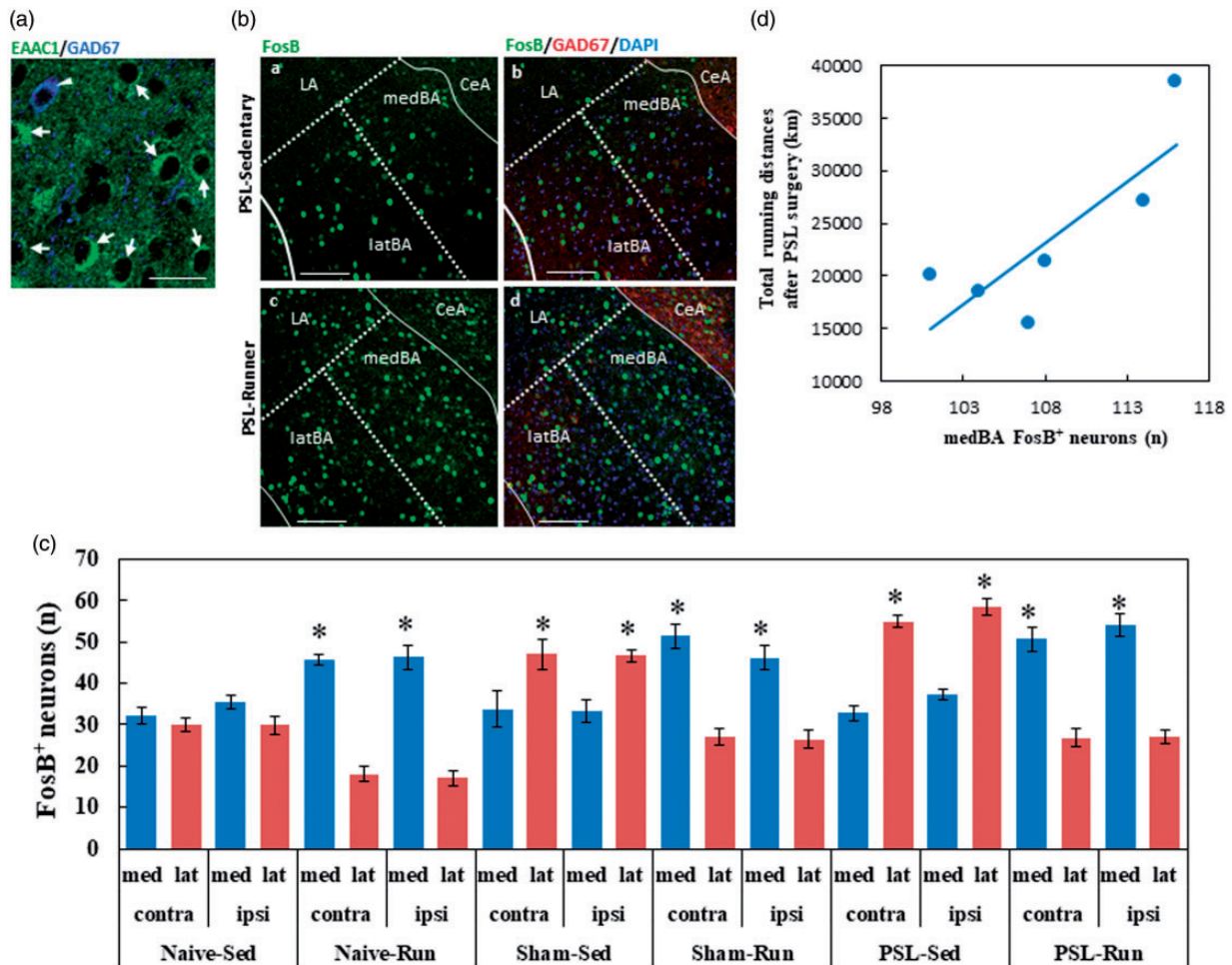
Figure 3. VR/PSL-induced changes of Glu neurons in the medBA and latBA. (A) Photomicrographs showing the neuronal types in the BA. Many EAAC1$^+$ Glu neurons (green, arrows) and a few GAD67$^+$ GABA neurons (blue, an arrowhead) were detected by dual immunostaining on the BA. Bar=30 μm. (B) Photomicrographs showing FosB$^+$ activated Glu neurons (green) and GAD67$^+$ GABA neurons (red) in the BA of PSL-Sedentary (a, b) and PSL-Runner (c, d) mice. The increased number of activated Glu neurons was observed in the medBA compared to the latBA in PSL-Runner mice, while these in PSL-Sedentary mice indicated the inverse pattern. LA: the lateral Amyg, medBA: the medial basal Amyg, latBA; the lateral basal Amyg, CeA: central nuclei of Amyg, Bars = 80 μm. (C) A bar chart showing the numbers of activated Glu neurons (GAD67$^-$ FosB$^+$) in the medBA and the latBA in each group. As shown in Figure 1(a), a square of 200 μm × 200 μm in size was placed on the medBA or the latBA on microscopic images, and GAD67$^-$ FosB$^+$ neurons per square were counted. Except for Naive-Sedentary, the activated Glu neurons in Naive-Run, Sham-Run and PSL-Run were significantly increased in the medBA compared to the latBA, while those in Sham-Sed and PSL-Sed were significantly increased in the latBA than those in the medBA (n = 6, *p < 0.01). (D) A significant positive correlation was noted between total running distances during two weeks after PSL operation and the number of activated Glu (GAD67$^-$ FosB$^+$) neurons in PSL-Runner mice (R = 0.813, n = 6, p < 0.05).

R = 0.835, n = 6, p < 0.05) and the CeL (Figure 4(h), R = 0.839, n = 6, p < 0.05), indicating that inactivation of GABA neurons in the CeA may be a factor to determine an intensity of neuropathic pain.

The NAc lateral shell-projecting BA-Glu neurons in runner mice

Using retrograde tracing and FosB immunostaining, we investigated whether the NAc lateral shell-projecting BA-Glu neurons are activated by VR. Mice were placed in individual cages with a running wheel at the start of the experiment, and after 13 days (Pre1 d), the running distance increased to 15528.47 ± 1119.07 m/day, as shown in Figure 5(a). A retrograde tracer, Retrobeads Red (RBR), was unilaterally injected into the left side of the NAc lateral shell, as described in Methods, and the RBR-injected mice then continued VR for 2 weeks (Figure 5(A) and (B)). Although the injection of RBR markedly decreased the running distance at day 1 post-injection (1 d: 3445.49 ± 973.82 m/day), the running distances gradually increased thereafter until day 14 post-injection (14 d: 13289.47 ± 1318.03 m/day) (Figure 5(A)). The brainstems in seven mice in which
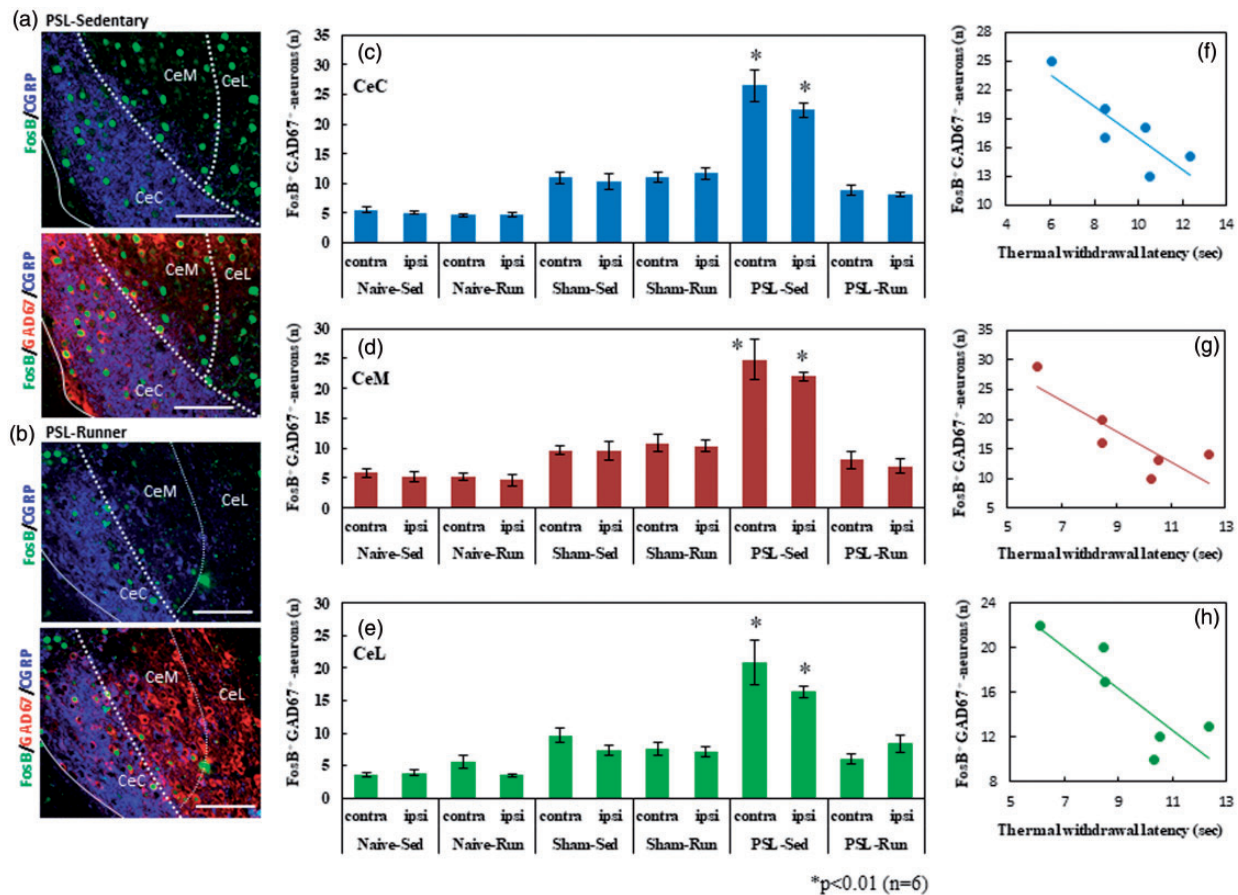
Figure 4. VR/PSL-induced changes of GABA neurons in the CeA subdivisions.
Photomicrographs showing the immunoreactivities for FosB (green), GAD67 (red) and CGRP (blue) antibodies in the CeA subdivisions in PSL-Sedentary (a) and PSL-Runner mice (b). Many activated GABA (GAD67$^+$ FosB$^+$) neurons were detected in the CeA subdivisions of PSL-Sedentary mice compared to those of PSL-Runner mice. CeC: the capsular division of CeA, CeL: lateral division of CeA, CeM: medial division of CeA. Bars = 70 μm. A bar chart showing the numbers of activated GABA neurons (GAD67$^+$ FosB$^+$) in the CeC (c), CeM (d) and CeL (e) in each group. As shown in Figure 1(a), a square of 100 μm × 100 μm in size was placed on the CeA subdivisions on microscopic images, and GAD67$^+$ FosB$^+$ neurons per square were counted. The activated GABA neurons in all CeA subdivisions were significantly increased in PSL-Sedentary compared to other groups (n = 6, *p < 0.01). Significant negative correlations were noted between thermal withdrawal latency and the number of activated GABA (GAD67$^+$ FosB$^+$) neurons in the CeC (F, R = 0.848, n = 6, p < 0.05), CeM (G, R = 0.835, n = 6, p < 0.05) and CeL (H, R = 0.839, n = 6, p < 0.05) in PSL-Runner mice.

RBR was precisely injected into the NAc lateral shell were used for further immunostaining.

Although RBR-incorporated neurons were bilaterally detected in the BA, more RBR$^+$ neurons were detected on the ipsilateral side than on the contralateral side of the injection (data not shown). Therefore, we performed further analysis on the ipsilateral side of the BA. We found that the proportion of RBR$^+$ neurons in the medBA (59.65 ± 3.2%, n = 7, p < 0.001) were significantly higher than that of the latBA (40.35 ± 3.2%), indicating that more Glu neurons in the medBA project into the NAc lateral shell in accordance with previous study[9] (Figure 5(C-a), and (D)). On immunostaining with FosB antibodies, we found mainly two distinct neuronal types, namely, NAc lateral shell-projecting activated Glu (RBR$^+$ FosB$^+$) and NAc lateral shell-non-projecting

activated Glu (RBR$^-$ FosB$^+$) neurons (Figure 5(C-b) and (C-c)). In the quantitative analysis, significantly many NAc lateral shell-projecting activated Glu neurons were detected in the medBA (70.9 ± 1.2%, n = 7, p < 0.001) compared with that of the latBA (29.1 ± 1.2%) (Figure 5(D)). These results indicated that VR can activate the NAc lateral shell-projecting the medBA-Glu neurons.

Discussion

Although EIH effects have been well documented in the pain model animals which performed treadmill running or VR, the brain mechanisms underlying induction and maintenance of EIH effects are not fully understood. The present results suggested that the VR in NPP
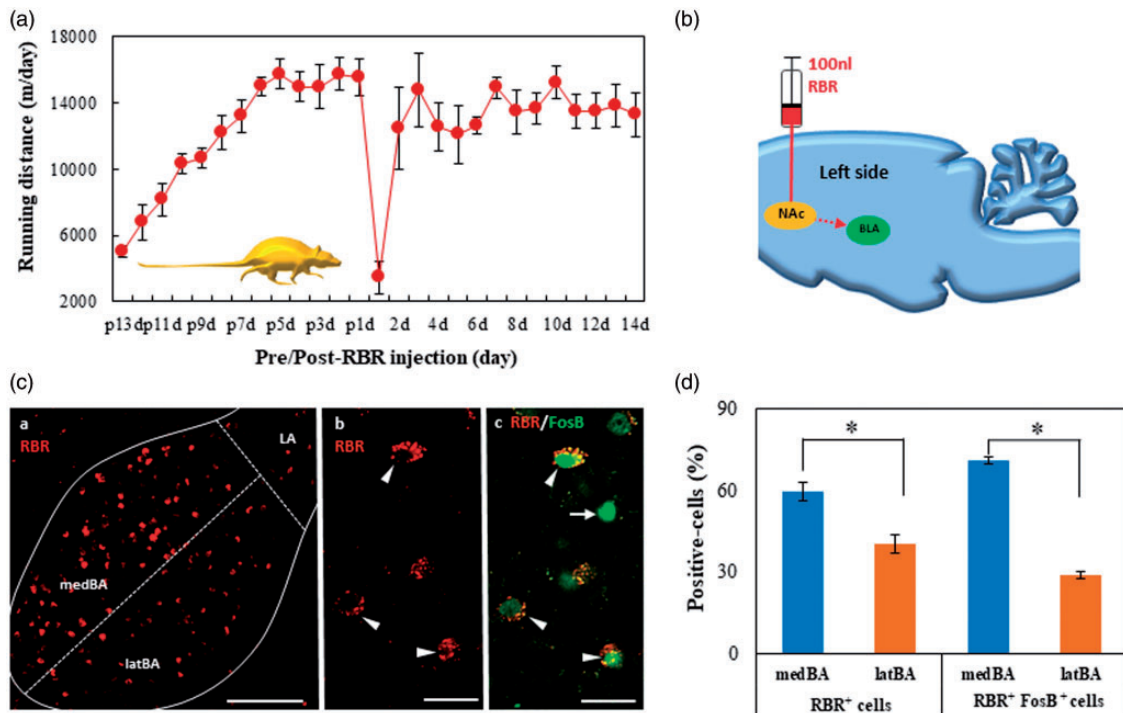
Figure 5. NAc lateral shell-projecting the BA-Glu neurons in Runner mice. (A) Changes in running distances in RBR-injected mice (n = 7). (B) After two weeks of VR, 50 nl of RBR was injected into the left side of the NAc lateral shell in mice, and RBR-injected mice continued VR for two more weeks. (C) Photomicrographs showing (a) positive signals for RBR (red) in the BA, (b, c) enlarged images of neurons with positive signals for RBR (red) and FosB (green) in the medBA. Arrowheads and an arrow indicate activated Glu (RBR$^+$ FosB$^+$) neurons projecting to the NAc lateral shell and activated Glu (RBR$^-$ FosB$^+$) neurons non-projecting to the NAc lateral shell, respectively. Bars: (a)= 150 μm, (b, c)=30 μm. (D) A bar chart showing the percentage of RBR$^+$ cells in the medBA or the latBA to RBR$^+$ cells in the BA (left side) and percentage of RBR$^+$ FosB$^+$ cells in the medBA or in the latBA to RBR$^+$ FosB$^+$ cells in the BA (right side) (n = 7, *p < 0.001).

condition may not only suppress negative emotions such as fear and anxiety closely related with pain chronication, but also arouse pleasant emotions to produce EIH effects.

The present study indicated that the decreased running distances following PSL were restored day by day by VR in accordance with our recent report, in which we demonstrated that VR of 2 weeks after surgery significantly improved pain behaviors.[4] Together with previous animal studies,[15,16,29–31] the present study confirmed availability of VR to produce EIH effects. In addition, we found a significant positive correlation between the total running distance after PSL-surgery, but not that during the whole experimental period, and thermal withdrawal latency, suggesting that the amount of VR after nerve injury is a critical factor to govern the analgesic level of EIH effects. VR has been well known to produce natural reward that can activate the mesolimbic reward system including the VTA-dopamine (DA) neurons.[23,32–34] Therefore, it clearly shows that the more active physical activity after nerve injury may cause the more activation of the mesolimbic reward system, which may contribute to the extinction of NPP-induced negative emotions such as fear, depression and anxiety.

We found that the number of activated Glu neurons was significantly increased in the medBA in all groups of runner mice including PSL-Runner mice, while those in the latBA showed higher levels in all groups of sedentary mice, suggesting that the Glu neurons mainly located in the medBA and latBA may play different roles each other. In addition, our tracer experiment showed that the Glu neurons in the medBA projecting to the NAc lateral shell are drastically activated by VR. It has been known that BLA projection neurons mediate both negative and positive emotions. For instance, selective activation of BLA neurons projecting to the NAc promotes reward seeking behavior, while selective activation of those projecting to the CeM induced fear-avoidance behavior.[35] Interestingly, Beyeler et al.[9] reported that BLA neurons projecting to the NAc were densely located in the medBA, while those projecting to the CeM were higher in the latBA compared to the medBA. In addition to these previous findings, we further showed that VR preferentially activates Glu neurons in the medBA projecting into the NAc, demonstrating that VR is an irreplaceable reward for PSL-mice, and consequently may be able to robustly produce positive emotions, thereby negating negative emotions including

aversion and fear induced by chronic pain. This idea may be supported by our results in which a positive correlation was observed between the number of FosB^{+} neurons in the medBA and total running distances after PSL-surgery. Contrarily, we found that PSL preferentially activated Glu neurons in the latBA projecting to the CeM. This seems to be reasonable, because it has been well known that the CeM together with the CeL play important roles as output regions in the CeA and work to produce and reinforce negative emotions associated with chronic pain.[6] Thus, both promotion of positive emotions and dissolution of negative emotions via activation of Glu neurons located in the medBA and projecting into the NAc may be a critical event to produce EIH effects.

We found that the numbers of activated GABA neurons in the CeA in Naive and Sham groups were maintained comparatively low levels, showing no significant differences among both groups. However, surprisingly, PSL operation caused significant increases of activated GABAergic neurons in all subdivisions, the CeC, CeM and CeL. Since the projection neurons from CeM and CeL to the hypothalamus, other limbic structures and brainstem regions, can induce negative emotions,[6] in addition to freezing response and autonomic symptoms, our results suggest that activated GABA neurons in the CeM and CeL may contribute to the development and maintenance of negative emotions such as fear and anxiety associated with neuropathic pain. On the other hand, the CeC neurons receive excitatory input from the external part of the PBN through the spino-parabranchial-amygdaloid pain pathway.[7] Therefore, the present results suggest that dramatic increase of activated GABA neurons in the CeC may be due to the increased nociceptive inputs derived from PSL surgery, which can also induce diverse changes including activations of astrocytes and microglia in the spinal dorsal horns.[36]

Interestingly, VR decreased the number of activated GABAergic neurons in all CeA subdivisions to almost the same levels as those of Naive and Sham groups. In addition, we found a significant positive correlation between thermal withdrawal latency and the number of FosB[+]/GAD67^{+} neurons in the CeC, CeM and CeL in the PSL-Runner mice. Furthermore, the fact that thermal withdrawal latency and total running distances after PSL surgery positively correlate, suggests that enhanced motivation to run and consequently increased voluntary running levels may work as unique stimuli to inhibit activation of GABA neurons in the CeA subdivisions. Previous studies provided possible mechanisms that can inactivate GABA neurons in the CeA following exercise. For example, treadmill running in rats that received a crush injury of sciatic nerve not only induces anti-inflammatory cytokines including interleukin-4 (IL-4)

and interleukin-5 (IL-5), but also suppress production of pro-inflammatory cytokines such as interleukin-1β (IL-1β) and tumor necrosis factor-α (TNF-α) via reduction of M1 macrophages in the injured sciatic nerves.[37] Therefore, significant decreases of activated GABA neurons in the CeC following VR may be induced by induction of anti-inflammatory cytokines and/or inhibition of pro-inflammatory cytokines in the injured sciatic nerves.

In addition to CeC-GABA neurons, we found that VR also suppresses activation of GABA neurons in the CeM and CeL subdivisions. CeL neurons are activated by inputs from Glu neurons in the BLA and GABA neurons in the ITC directly and from Glu neurons in the mPFC indirectly.[6] Sun et al.[38] reported that Glu neurons from the BLA project onto both mPFC-Glu neurons and -GABA interneurons. In NPP model animals, mPFC-Glu neurons receive enhanced feed-forward inhibition via parvalbumin expressing GABA interneurons, which may enhance output from the CeL via inhibition of ITC-GABA neurons, thereby contributing to the development and maintenance of pain behaviors. Contrarily, optogenetic activation of mPFC-Glu neurons reversed mechanical and thermal hypersensitivity in NPP model mice.[39] Although it should be investigated in the future whether mPFC-Glu neurons are activated and/or mPFC-GABA interneurons are inactivated by VR, these findings suggest that disinhibition of feed-forward inhibition by GABA interneurons in the mPFC following VR may be involved in the decrease of activated GABA neurons in the CeL. Similarly, we found significant decrease of activated GABA neurons located in the CeM following VR. In accordance with this change, our results indicated that PSL-Runner mice inhibit the number of activated Glu neurons in the latBA, which preferentially project into the CeM, suggesting that this is a possible mechanism to suppress activation of GABA neurons in the CeM. Thus, our results suggested that inactivation of GABA neurons in the CeA subdivisions which is induced by VR perhaps through different mechanisms may be critical events to actuate EIH effects.

Here we described that both promotion of positive emotions and relief of negative emotions via activation of Glu neurons in the medBA projecting to the NAc and inactivation of GABA neurons in the CeA subdivisions may constitute critical events to produce EIH effects. Amygdala plays a key role in fear learning and extinction,[40,41] and the CeA neurons are activated by enhanced inputs from the spino-parabrachio-amygdaloid pathway that play a role in fear learning.[42] Therefore, the present study also suggests that VR may be involved in fear extinction via inactivation of GABA neurons in the CeA subdivisions. Mutso et al.[43] reported the longer freezing times in the context fear extinction were observed in NPP model rats compared to those of

Sham operated rats. These findings raised a hypothesis in which physical exercise in NPP condition may accelerate disappearance of fear memories. This hypothesis is now being investigated in our laboratory, because we think that extinction of fear by physical exercise may be an important mechanism underling EIH effects. Further investigations focusing on the relationship between fear extinction and EIH effects may give us a vital clue to disclosing the underlying mechanisms of EIH.

Authors' Contribution

KK and ES planned this study. KK performed the behavioral experiments, the immunostainings and the image analysis. All authors contributed to the interpretation and discussion of results. Comments on the manuscript and approval of the final version were given by all authors.

Declaration of Conflicting Interests

The author(s) declared no potential conflicts of interest with respect to the research, authorship, and/or publication of this article.

Funding

ORCID iD

Katsuya Kami https://orcid.org/0000-0003-0467-5091

References

1. Koltyn KF, Brellenthin AG, Cook DB, Sehgal N, Hillard C, Mechanisms of exercise-induced hypoalgesia. *J Pain* 2014; 15: 1294–1304.
2. Senba E, Kami K. A new aspect of chronic pain as a lifestyle-related disease. *Neurobiol Pain* 2017; 1: 6–15.
3. Kami K, Tajima F, Senba E. Exercise-induced hypoalgesia: potential mechanisms in animal models of neuropathic pain. *Anat Sci Int* 2017; 92: 79–90.
4. Kami K, Tajima F, Senba E. Activation of mesolimbic reward system via laterodorsal tegmental nucleus and hypothalamus in exercise-induced hypoalgesia. *Sci Rep* 2018; 8: 11540.
5. Ji G, Neugebauer V. Pain-related deactivation of medial prefrontal cortical neurons involves mGluR1 and $GABA_A$ receptors. *J Neurophysiol* 106; 2011: 2642–2652.
6. Thompson JM, Neugebauer V. Cortico-limbic pain mechanisms. *Neurosci Lett* 2019; 702: 15–23.
7. Thompson JM, Neugebauer V. Amygdala plasticity and pain. *Pain Res Manag* 2017; 2017: 8296501.
8. Beyeler A, Namburi P, Glober GF, Simonnet C, Calhoon GG, Conyers GF, Luck R, Wildes CP, Tye KM. Divergent routing of positive and negative information from the amygdala during memory retrieval. *Neuron* 2016; 90: 348–361.
9. Beyeler A, Chang CJ, Silvestre M, Lévêque C, Namburi P, Wildes CP, Tye KM. Organization of valence-encoding and projection-defined neurons in the basolateral amygdala. *Cell Rep* 2018; 22: 905–918.
10. Cai YQ, Wang W, Paulucci-Holthauzen A, Pan ZZ. Brain circuits mediating opposing effects on emotion and pain. *J Neurosci* 2018; 38: 6340–6349.
11. Seltzer Z, Dubner R, Shir Y. A novel behavioral model of neuropathic pain disorders produced in rats by partial sciatic nerve injury. *Pain* 1990; 43: 205–218.
12. Imbe, H, Okamoto, K., Donishi, T, Senba, E, Kimura A. Involvement of descending facilitation from the rostral ventromedial medulla in the enhancement of formalin-evoked nocifensive behavior following repeated forced swim stress. *Brain Res* 2010; 1329:103–112.
13. Zheng J, Jiang YY, Xu LC, Ma LY, Liu FY, Cui S, Cai J, Liao FF, Wan Y, Yi M. Adult hippocampal neurogenesis along the dorsoventral axis contributes differentially to environmental enrichment combined with voluntary exercise in alleviating chronic inflammatory pain in mice. *J Neurosci* 2017; 37: 4145–4157.
14. Chen C, Nakagawa S, Kitaichi Y, An Y, Omiya Y, Song N, Koga M, Kato A, Inoue T, Kusumi I. The role of medial prefrontal corticosterone and dopamine in the antidepressant-like effect of exercise. *Psychoneuroendocrinology* 2016; 69: 1–9.
15. Pitcher MH, Tarum F, Rauf IZ, Low LA, Bushnell C. Modest amounts of voluntary exercise reduce pain- and stress-related outcomes in a rat model of persistent hind limb inflammation. *J Pain* 2017; 18: 687–701.
16. Brito RG, Rasmussen LA, Sluka KA. Regular physical activity prevents development of chronic muscle pain through modulation of supraspinal opioid and serotonergic mechanisms. *Pain Rep* 2017; 2: e618.
17. Grace PM, Fabisiak TJ, Green-Fulgham SM, Anderson ND, Strand KA, Kwilasz AJ, Galer EL, Walker FR, Greenwood BN, Maier SF, Fleshner M, Watkins LR. Prior voluntary wheel running attenuates neuropathic pain. *Pain* 2016; 157: 2012–2023.
18. Binder E, Droste SK, Ohl F, Reul JM. Regular voluntary exercise reduces anxiety-related behaviour and impulsiveness in mice. *Behav Brain Res* 2004; 155: 197–206.
19. Duman CH, Schlesinger L, Russell DS, Duman RS. Voluntary exercise produces antidepressant and anxiolytic behavioral effects in mice. *Brain Res* 2008; 1199: 148–158.
20. Salam JN, Fox JH, Detroy EM, Guignon MH, Wohl DF, Falls WA. Voluntary exercise in C57 mice is anxiolytic across several measures of anxiety. *Behav Brain Res* 2009; 197: 31–40.
21. McDonald A. *Cell types and intrinsic connections of the amygdala. The amygdala: Neurobiological aspects of emotion, memory, and mental dysfunction*. New York: Wiley-Liss, 1992, pp. 67–96.
22. Spampanato J, Polepalli J, Sah P. Interneurons in the basolateral amygdala. *Neuropharmacology* 2011; 60: 765–773.

23. Greenwood BN, Foley TE, Le TV, Strong PV, Loughridge AB, Day HE, Fleshner M. Long-term voluntary wheel running is rewarding and produces plasticity in the meso-limbic reward pathway. *Behav Brain Res* 2011; 217: 354–362.

24. Duvarci S, Pare D. Amygdala microcircuits controlling learned fear. *Neuron* 2014; 82: 966–980.

25. Kim J, Zhang X, Muralidhar S, LeBlanc SA, Tonegawa S. Basolateral to central amygdala neural circuits for appeti-tive behaviors. *Neuron* 2017; 93: 1464–1479.

26. McCullough KM, Morrison FG, Hartmann J, Carlezon WA Jr, Ressler KJ. Quantified coexpression analysis of central amygdala subpopulations. *eNeuro* 2018; 5: 1–12.

27. Shinohara K, Watabe AM, Nagase M, Okutsu Y, Takahashi Y, Kurihara H, Kato F. Essential role of endogenous calcitonin gene-related peptide in pain-associated plasticity in the central amygdala. *Eur J Neurosci* 2017; 46: 2149–2160.

28. Franklin KBJ, Paxinos G. *The mouse brain in stereotaxic coordinates, compact, third edition: The coronal plates and diagrams.* Cambridge: Academic Press, 2008.

29. Groover AL, Ryals JM, Guilford BL, Wilson NM, Christianson JA, Wright DE. Exercise-mediated improve-ments in painful neuropathy associated with prediabetes in mice. *Pain* 2013; 154: 2658–2667.

30. Lima LV, DeSantana JM, Rasmussen LA, Sluka KA. Short-duration physical activity prevents the development of activity-induced hyperalgesia through opioid and sero-toninergic mechanisms. *Pain* 2017; 158: 1697–1710.

31. Sluka KA, O'Donnell JM, Danielson J, Rasmussen LA. Regular physical activity prevents development of chronic pain and activation of central neurons. *J Appl Physiol* 2013; 114: 725–733.

32. Herrera JJ, Fedynska S, Ghasem PR, Wieman T, Clark PJ, Gray N, Loetz E, Campeau S, Fleshner M, Greenwood BN. Neurochemical and behavioural indices of exercise reward are independent of exercise controllability. *Eur J Neurosci* 2016; 43: 1190–1202.

33. Boekhoudt L, Omrani A, Luijendijk MC, Wolterink-Donselaar IG, Wijbrans EC, van der Plasse G, Adan RA. Chemogenetic activation of dopamine neurons in the ventral tegmental area, but not substantia nigra, induces hyperactivity in rats. *Eur Neuropsychopharmacol* 2016; 26: 1784–1793.

34. Belke TW, Wagner JP. The reinforcing property and the rewarding aftereffect of wheel running in rats: a combina-tion of two paradigms. *Behav Processes* 2005; 68: 165–172.

35. Namburi P, Beyeler A, Yorozu S, Calhoon GG, Halbert SA, Wichmann R, Holden SS, Mertens KL, Anahtar M, Felix-Ortiz AC, Wickersham IR, Gray JM, Tye KM. A circuit mechanism for differentiating positive and negative associations. *Nature* 2015; 520: 675–678.

36. Kami K, Taguchi S, Tajima F, Senba E. Histone acetyla-tion in microglia contributes to exercise-induced hypoalge-sia in neuropathic pain model mice. *J Pain* 2016; 17: 588–599.

37. Bobinski F, Teixeira JM, Sluka KA, Santos ARS. Interleukin-4 mediates the analgesia produced by low-intensity exercise in mice with neuropathic pain. *Pain* 2018; 159: 437–450.

38. Sun T, Song Z, Tian Y, Tian W, Zhu C, Ji G, Luo Y, Chen S, Wang L, Mao Y, Xie W, Zhong H, Zhao F, Luo MH, Tao W, Wang H, Li J, Li J, Zhou J, Wang K, Zhang Z. Basolateral amygdala input to the medial prefrontal cortex controls obsessive-compulsive disorder-like checking behavior. *Proc Natl Acad Sci U S A* 2019; 116: 3799–3804.

39. Zhang Z, Gadotti VM, Chen L, Souza IA, Stemkowski PL, Zamponi GW. Role of prelimbic GABAergic circuits in sensory and emotional aspects of neuropathic pain. *Cell Rep* 2015; 12: 752–759.

40. Hartley CA, Phelps EA. Changing fear: the neurocircuitry of emotion regulation. *Neuropsychopharmacology* 2010; 35: 136–146.

41. Phelps EA, LeDoux JE. Contributions of the amygdala to emotion processing: from animal models to human behav-ior. *Neuron* 2005; 48: 175–187.

42. Palmiter RD. The parabrachial nucleus: CGRP neurons function as a general alarm. *Trends Neurosci* 2018; 41: 280–293.

43. Mutso AA, Radzicki D, Baliki MN, Huang L, Banisadr G, Centeno MV, Radulovic J, Martina M, Miller RJ, Apkarian AV. Abnormalities in hippocampal functioning with persistent pain. *J Neurosci* 2012; 32: 5747–5756.